FILLET WELD STRESS USING FINITE ELEMENT METHODS

Terry F. Lehnhoff
University of Missouri-Rolla

Gerald W. Green
University of Missouri-Rolla

SUMMARY

Average elastic Von Mises equivalent stresses were calculated along the throat of a single lap fillet weld. The average elastic stresses were compared to initial yield as well as to plastic instability conditions to modify conventional design formulas so that they can be used to predict either extreme of failure by yielding. A new multiplying factor for the conventional design formulas is presented. The factor is a linear function of the thicknesses of the parent plates attached by the fillet weld.

INTRODUCTION

In theoretical analyses of stresses in welds, approximations have not only been traditionally accepted but have been considered appropriate. Much of the justification for this has been based on the presumption that analytical means for accurate solutions are not available. Furthermore, the limited quality control that is possible with many welding processes has supported this viewpoint. Welding technology is, however, steadily improving along with the quality control that is necessary to ensure consistency as well as reliably welded joints. This improvement will continue as welding becomes an even more significant part of future manufacturing processes.

The purpose of the present investigation was to establish more precise design formulas for single lap fillet welds subjected to tensile loading. The study has revealed a complexity in what appears to be a relatively simply geometry (fig. 1). In addition, it indicated that variations in the thicknesses of the welded plates have an influence on such welds. Different plate thicknesses affect the geometry as well as the load paths. The change in geometry is rather obvious, but the additional bending load, which is a natural consequence of the change in geometry, has not been considered in the conventional theory.

BASIC THEORY

Because the throat area of a weld as indicated by line BD in figure 1 is the minimum area through which loads must be transferred, it is the most probable area of failure. Leg BC is loaded predominantly in shear, whereas leg BE is primarily in tension. The throat must then be subjected to a combination of tension and shear. Shigley and Mitchell (ref. 1) showed that the largest principal stress on a throat area is defined as

$$\sigma_1 = 1.618(F/h\ell) , \qquad (1)$$

and the maximum shear stress as

$$\tau_{max} = 1.118(F/h\ell) \tag{2}$$

in which F is the applied load, ℓ the length of the weld in a direction normal to the page, and h the leg length. These stresses are calculated as averages for the entire throat. Norris (ref. 2), Salakian and Claussen (ref. 3), and Bagci (ref. 4) showed that the stresses vary significantly along both legs and that the throat has a large stress concentration at point B. Thus, although equations (1) and (2) are known to give average results, Shigley and Mitchell (ref. 1) noted that for design purposes, it is customary to base the shear stress on the throat area and to neglect the normal stress altogether. On this basis, the equation for average shear stress becomes

$$\tau = 1.414(F/h\ell) \tag{3}$$

and τ from equation (3) is 1.27 times greater than from equation (2). Obviously, an unknown safety factor has been incorporated in equation (3).

The present study brought out the fact that there is a logical rationale for a multiplying factor somewhat different than the one used in equation (3). Because the failure of mechanical components from either static or fatigue loading was shown by Shigley and Mitchell (ref. 1) to be related to the Von Mises-Hencky equivalent stress, it is used extensively in the discussion which follows.

If it is assumed as in equation (3) that the throat is subjected to pure shear, then the equivalent Von Mises stress can be shown to be

$$\sigma = \sqrt{3}\ 1.414(F/h\ell) = 2.449(F/h\ell). \tag{4}$$

In the present investigation, the finite element method was used to determine the actual distribution of the Von Mises stresses along the throat for several weld configurations. Averages of the results from elastic analyses were obtained, and these were compared with the results from some plastic analyses.

MODELS

Models were prepared, and analyses were performed by senior mechanical engineering students at the University of Missouri-Rolla. The finite element method was used to develop the models shown in figures 1 and 2. Several types and refinements of meshes were used at various stages of the work. Four-node quadrilateral and three-node triangular elements as well as eight-node quadrilateral and six-node triangular elements were used in the models. In each model, elastic analyses were performed with the element dimensions varying from 0.0635 (0.025) in most of the weld to 0.254 mm (0.010 in.) in the area of the most significant stress concentration (point B in fig. 1). For the elastic analyses, the maximum number of nodes was 2121, and the maximum number of elements was 806. For the plastic analyses, the maximum number of nodes was 411, and the maximum number of elements was 160. The maximum computer time on an IBM 4341 for the elastic analyses was 92 min, and the maximum for the plastic analyses was 10 min. Plastic analyses for which a refined mesh was used required almost four hours and were deemed impractical for multiple analyses.

The grid size was selected so that after sufficient refinement in the area of point B the nodal stresses from all elements surrounding a given node were the same to at least one significant figure. Point B was an exception because of the steep stress gradients.

ELASTIC ANALYSIS

Elastic studies were performed for plate thicknesses varying from 6.35 (0.25) to 22.22 mm (0.875 in.) in 3.18 mm (0.125 in.) increments. The weld leg length was kept constant at 6.35 mm (0.25 in.) for all plate thicknesses. Only the data for models 1 (Green), 2 (Morlock), and 3 (O'Brian) as defined in figure 1 have been shown in subsequent figures. Similar results were obtained for the other models.

Three load and constraint configurations were selected. The first one, which is shown in figure 2a (Case 1), was an attempt to subject the weld as nearly as possible to a direct load without a moment. Complete elimination of any moment would have been desirable but was impossible for the unsymmetrical geometry of the configuration. The loading and restraining conditions for practical applications are shown in figures 2b (Case 2) and 2c (Case 3). These are considered more realistic, because the loads in most physical components would be uniformly transferred through the thickness.

Because the results in Case 3 for symmetric geometry and loading were not significantly different from Case 1, they are not discussed in detail here.

Figure 3 shows a deformed plot of a simplified version of Case 1. It illustrates that although the loading and restraints were aligned, the unsymmetrical geometry caused the weld to rotate somewhat.

Figures 4a-4c show the general trends of the stress contours for maximum principal stress, minimum principal stress and maximum shear stress for the same model and load case as shown in figure 3. These are representative of the stress distribution throughout the weld.

Figure 5 shows the distribution of the Von Mises equivalent stress along the weld throat (BD in fig. 1) for Case 1. Figure 6 shows the same Von Mises equivalent stress as figure 5. The large stress at point B has been omitted to show more clearly the variations occasioned by the plate thicknesses in the various models.

Figure 7 shows the distribution of the Von Mises equivalent stress along the throat for Case 2. Figure 8 shows the same Von Mises stress as figure 7, and, again, the large stress at point B has been omitted to show the variations occasioned by the plate thicknesses in the various models.

Figures 5 and 7 are of different scales because of the large stresses at point B. However, figures 6 and 8 are of the same scale and can be overlayed for the purpose of comparing the effects of the loads of Cases 1 and 2.

PLASTIC ANALYSIS

Elastic perfectly plastic analyses were conducted for an AWS E80XX electrode with a tensile strength of 552 MPa (80 kpsi), a yield strength of 462 MPa (67 kpsi) and an assumed identical parent plate material. In general, the calculations were performed with increasing load increments until the strength became unstable.

The less refined models with nominal element dimensions of 0.635 mm (0.025 in.) were used in the plastic studies. This was necessary, because the iterative solution procedure was more demanding of computer resources. Figures 9, 10 and 11 show the development of the plastic zones as the load on a weld of unit length was increased to the point of instability. The results in figure 9 are for model 1 (Green) with Case 2 loading. The results in figure 10 are for model 2 (Morlock) with Case 2 loading, whereas the results in figure 11 are for model 3 (O'Brian) with Case 2 loading. Similar results were also obtained for the other models defined in figure 1.

DISCUSSION

The average elastic Von Mises stresses along the throat shown in figures 5 through 8 are suggested as being more indicative of failure than the traditional relationship given by equation (3). Failure in the static sense can be either the initiation of yielding or the point of plastic instability where a weld has essentially yielded along the entire length of its throat.

For the models defined in figure 1 in each of the elastic analyses, the load was taken as 4.448 N (1.0 lb) acting on a weld of leg length 6.35 mm (0.25 in.) and length 25.4 mm (1.0 in.). For these conditions, the conventional theory as expressed by equation (4) indicates an average Von Mises stress of 67538 Pa (9.796 psi). Furthermore, the conventional theory does not include plate thickness as a variable.

With Case 1 (fig. 2) and 4.448 N (1.0 lb) loading, figures 5 and 6 show that the stress does not vary significantly with plate thickness. The average stress was determined to be 58086 Pa (8.425 psi). With Case 2 (fig. 2) and 4 448 N (1.0 lb) loading, the average Von Mises stress was determined to be 105699 Pa (15.331 psi) for model 1, 178470 Pa (25.886 psi) for model 2 and 248207 Pa (36.001 psi) for model 3. Case 2 loading thus shows a definite deviation from conventional theory.

If it is assumed that the finite element results indicate a correct average Von Mises stress, then the conventional equation should be multiplied by 58086/67538 = 0.86 for Case 1 type loading. If, instead of assuming pure shear as in the conventional approach, it is assumed that the Von Mises stress corresponding to equations (1) and (2) is appropriate, then a multiplier of 0.82 for equation (4) should be the result. The most accurate conventional theory, therefore, deviates by only 4 percent from the finite element method. However, by expressing equations (3) and (4) as they should be applied for Case 1 (fig. 2) loading, one has

$$\tau = 0.86(1.414)(F/h\ell) = 1.22(F/h\ell) \tag{5}$$

and

$$\sigma = 0.86(2.449)(F/h\ell) = 2.11(F/h\ell). \tag{6}$$

Now the multipliers in equations (3) and (4) for Case 2 (fig. 2) loading should be 1.57 for model 1, 2.64 for model 2 and 3.68 for model 3. Thus, conventional theory is inadequate when the plates are thicker and the load is distributed.

The comparison given above in equations (5) and (6) shows what is necessary to make the conventional formulas for the average shear stress on a plastic weld throat and the corresponding Von Mises equivalent normal stress agree with more accurate calculations of those stresses. However, the objective of the design engineer is to

be able to predict not only the beginning of yielding but the fully plastic instability condition as well. Consequently, one must relate equations (5) and (6) to these yield conditions.

Plastic analyses allow one to adjust the conventional formulas (eqs. (3) through (6)) so that either initial yielding or plastic instability can be predicted. To determine the constant for the initiation of yielding, it is assumed that the load at which yielding first occurs corresponds to the load when an element in the parent material immediately to the left of the corner at point B (fig. 1) has experienced general yielding, and the corner element in the weld has just started to yield. It was noted during the numerical experiments that at this load the weld also begins to yield in the region of point D. For each of the models, this load was divided by the load at which plastic instability occurred. The average of these ratios was approximately 2/3 for all of the models for both Case 1 and Case 2 loading. None of the models varied significantly from the 2/3 value. Thus, the ratio of the load for initial yielding to the load for plastic instability is relatively constant for the models and for the material illustrated in figures 9 through 11 as well as for the others noted in the table of figure 1 for both Case 1 and Case 2 loading.

It remains to show how the average elastic Von Mises equivalent stress relates to either initial yielding or plastic instability. Figures 9 through 11 show the progression of the plastic deformation zones for three of the models. As noted earlier, the parent material and weld were assumed to be identical with a yield strength of 462 MPa (67 kpsi). For this material and an elastic perfectly plastic assumption, the various models became unstable at the next load increment. That is in figure 9 for model 1, the instability is shown to have occurred between 17.8 (4.0) and 18.7 kN (4.2 kips), and in figure 10 for model 2 the instability is shown to have occurred between 10.7 (2.4) and 11.6 kN (2.6 kips), whereas in figure 11, the instability is shown to have occurred between 8.0 (1.8) and 8.9 kN (2.0 kips). Furthermore, for Case 1 loading, the instability is shown to have occurred at approximately the same load for all models and was between 33.8 (7.6) and 35.5 kN (8.0 kips).

The loads at which the average elastic Von Mises stress equals the yield strength of the material were determined. This was done on the presumption that general plastic yielding and instability occur when the average elastic Von Mises equivalent stress is equal to the yield strength of the material. To determine these loads, the yield strength was divided by the average elastic Von Mises stresses as indicated in figures 5 through 8. For Case 2 loading for model 1, the ratio is 19.4 kN (4.37 kips), and for model 2, the ratio is 11.4 kN (2.59 kips), whereas for model 3, the ratio is 8.3 kN (1.86 kips). For Case 1 loading, the load when the average Von Mises stress equaled the material yield strength was 35.4 kN (7.95 kips), and it was approximately the same for all models. The loads are compared in Table 1 where it is evident that the average elastic Von Mises stress along the throat is an excellent indicator of plastic instability.

Because equation (6) permits a more accurate calculation of the average Von Mises equivalent stress along the throat of the weld, it also predicts the fully plastic instability condition when the calculated Von Mises stress equals the yield strength of the material. Furthermore, equation (6) can be used to predict the onset of yielding when the calculated stress equals 2/3 of the material yield strength.

To obtain a design equation for the onset of yielding, equation (6) can be multiplied by 3/2 as follows:

$$\sigma = (3/2)(0.86)(2.449)(F/h\ell) = 3.16(F/h\ell). \qquad (7)$$

When the applied load F is such that σ equals the material yield strength, then for Case 1 loading, the weld will experience the initiation of yielding. For Case 2 loading, the 0.86 factor must be replaced by 1.57, 2.64, and 3.68 for models 1, 2, and 3 respectively. All of the constants are listed in Table 2 The data for load Case 2 from Table 2 are plotted in figure 12. Because the constants are related linearly, one can write equation (7) as follows:

$$\sigma = f(F/h\ell) \tag{8}$$

in which

$$f = 3.88(A/h) + 1.90 \tag{9}$$

for Case 2, and A/h, the plate thickness to weld leg length ratio, must be greater than or equal to one. Equations (7) and (8) provide the basis for the design of single lap fillet joints for the initiation of yielding of the weld throat. Equation (6) allows for fully plastic design. However, the influence of strain hardening will usually make equation (6) somewhat conservative.

REFERENCES

1. Shigley, J. E.; and Mitchell, L. D.: Mechanical Engineering Design. Fourth Edition, McGraw Hill 1983, p. 417.

2. Norris, C. H.: Photoelastic Investigation of Stress Distribution in Transverse Fillet Welds. Welding Journal, vol. 24, 1945, p. 557.

3. Salakian, A. G.; and Claussen, G. E.: Stress Distribution in Fillet Welds; A Review of the Literature. Welding Journal, vol. 16, May 1973, pp. 1-24.

4. Bagci, C.: Finite Stress Elements and Applications in Machine Design. OSU Applied Mechanisms Conference, Denver, October 1979.

TABLE 1.-RELATION OF AVERAGE ELASTIC VON MISES AND PLASTIC LOADS

LOAD CASE	PLATE THICKNESS mm (in.)	Load for Average Von Mises Stress Equal to Material Yield Strength kN (kips)	Load Range for Plastic Instability kN (kips)
1	All	35.4 (7.95)	33.8 (7.6) - 35.6 (8.0)
2	6.35 (0.25)	19.4 (4.37)	17.8 (4.0) - 18.7 (4.2)
2	12.70 (0.50)	11.5 (2.59)	10.7 (2.4) - 11.6 (2.6)
2	19.05 (0.75)	8.3 (1.86)	8.0 (1.8) - 8.9 (2.0)

TABLE 2.-CONSTANTS FOR EQUATION 7

LOAD CASE	PLATE THICKNESS mm (in.)	CONSTANTS FOR EQUATION 7
1	All	3.16
2	6.35 (0.25)	5.76
2	12.70 (0.50)	9.70
2	19.05 (0.75)	13.52

LIST OF FIGURES

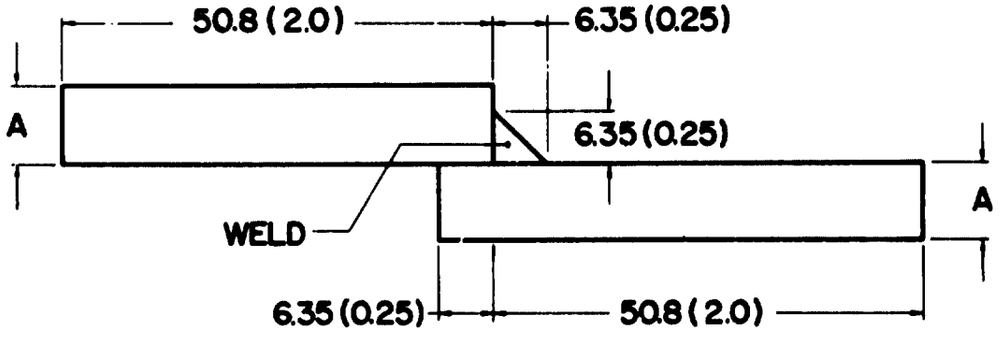

NOTE ALL DIMENSIONS IN mm (in.)

MODEL	A
1 (GREEN)	6.35 (0.250)
(ILISEVIC)	9.52 (0.375)
2 (MORLOCK)	12.70 (0.500)
(ROGAN)	15.88 (0.625)
3 (O BRIAN)	19.05 (0.750)
(BOHR)	22.22 (0.875)

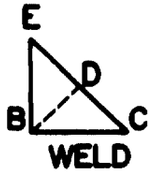

BC - SHEAR LEG
BD - THROAT
BE - TENSION LEG

FIGURE 1 FILLET WELD MODEL DIMENSIONS

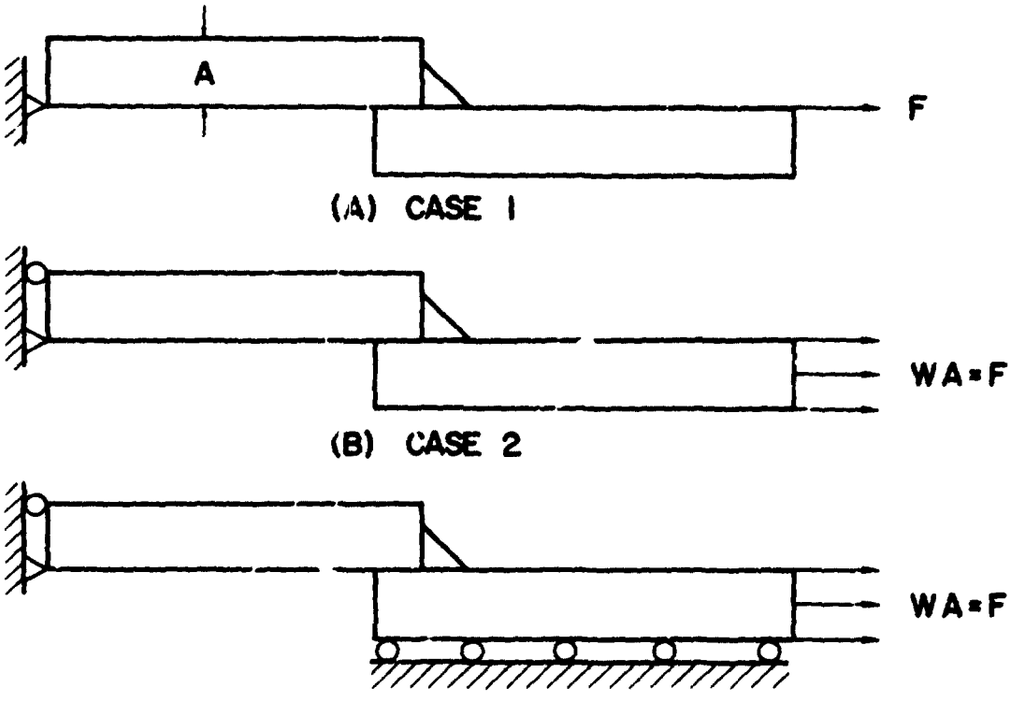

FIGURE 2 LOAD AND RESTRAINT CASES

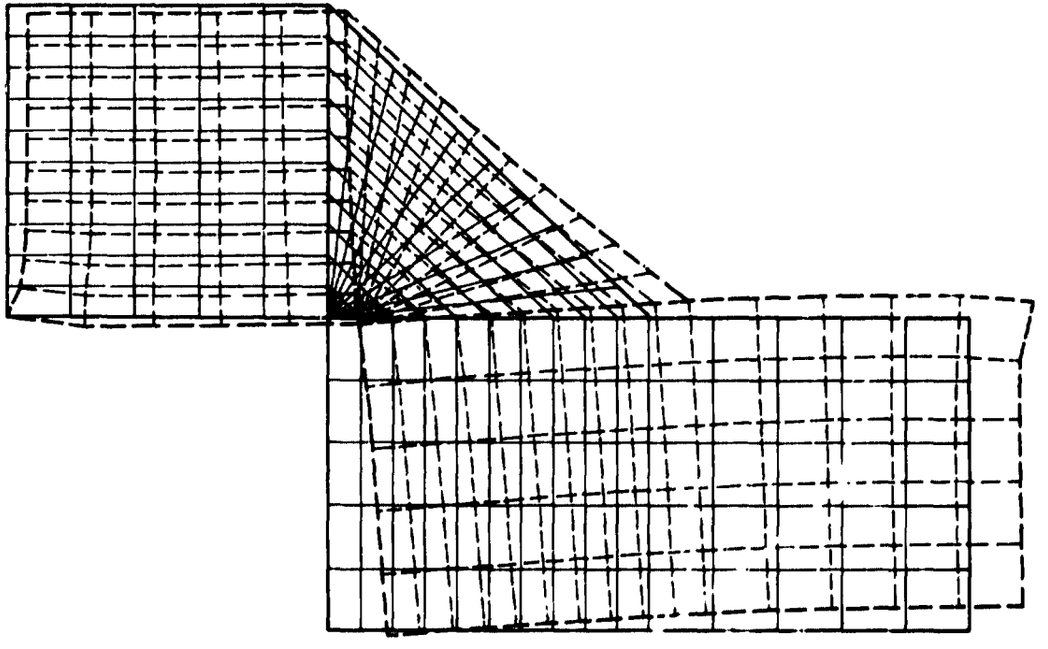

FIGURE 3 DEFORMED GEOMETRY, CASE I

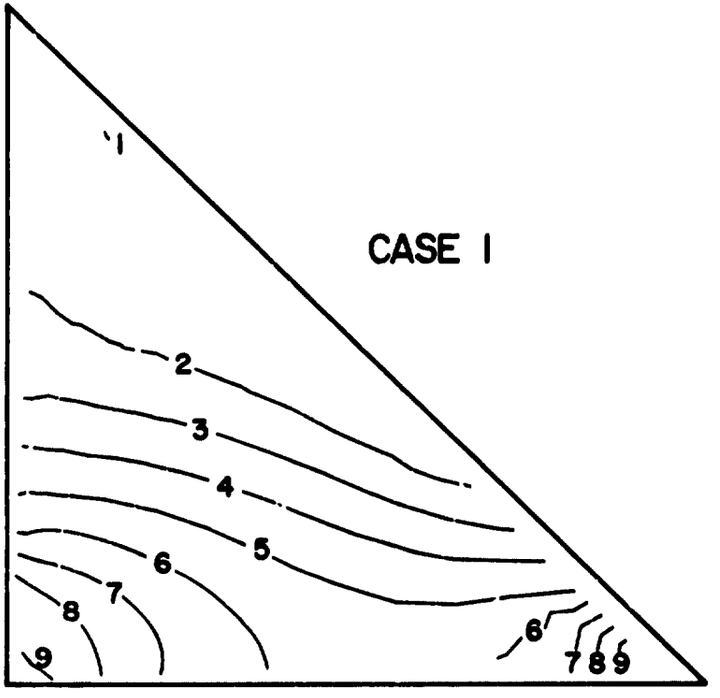

FIGURE 4a TYPICAL MAXIMUM PRINCIPAL STRESS

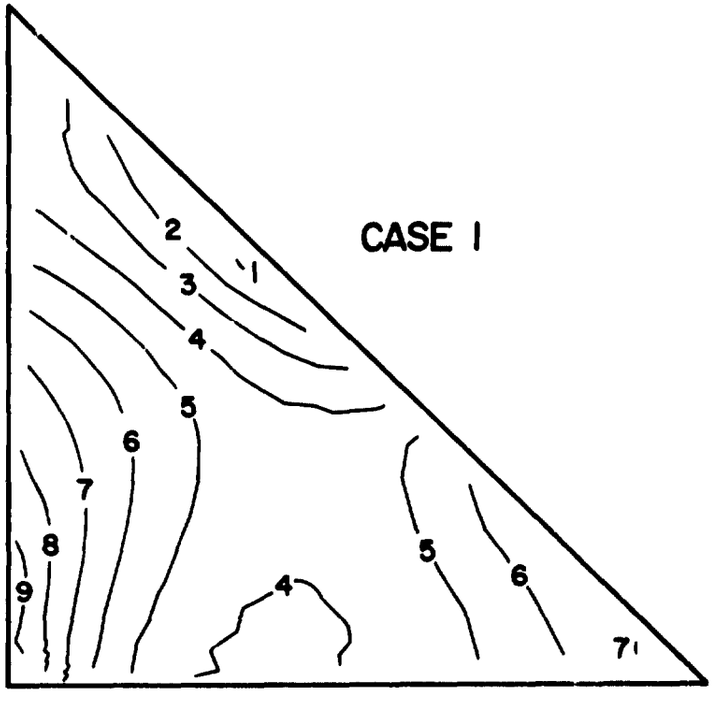

FIGURE 4b TYPICAL MINIMUM PRINCIPAL STRESS

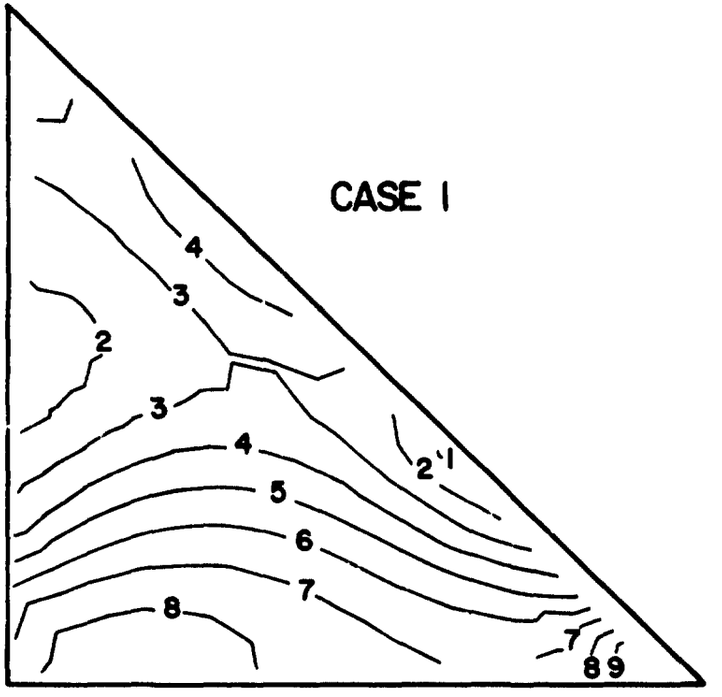

FIGURE 4c TYPICAL MAXIMUM SHEAR STRESS

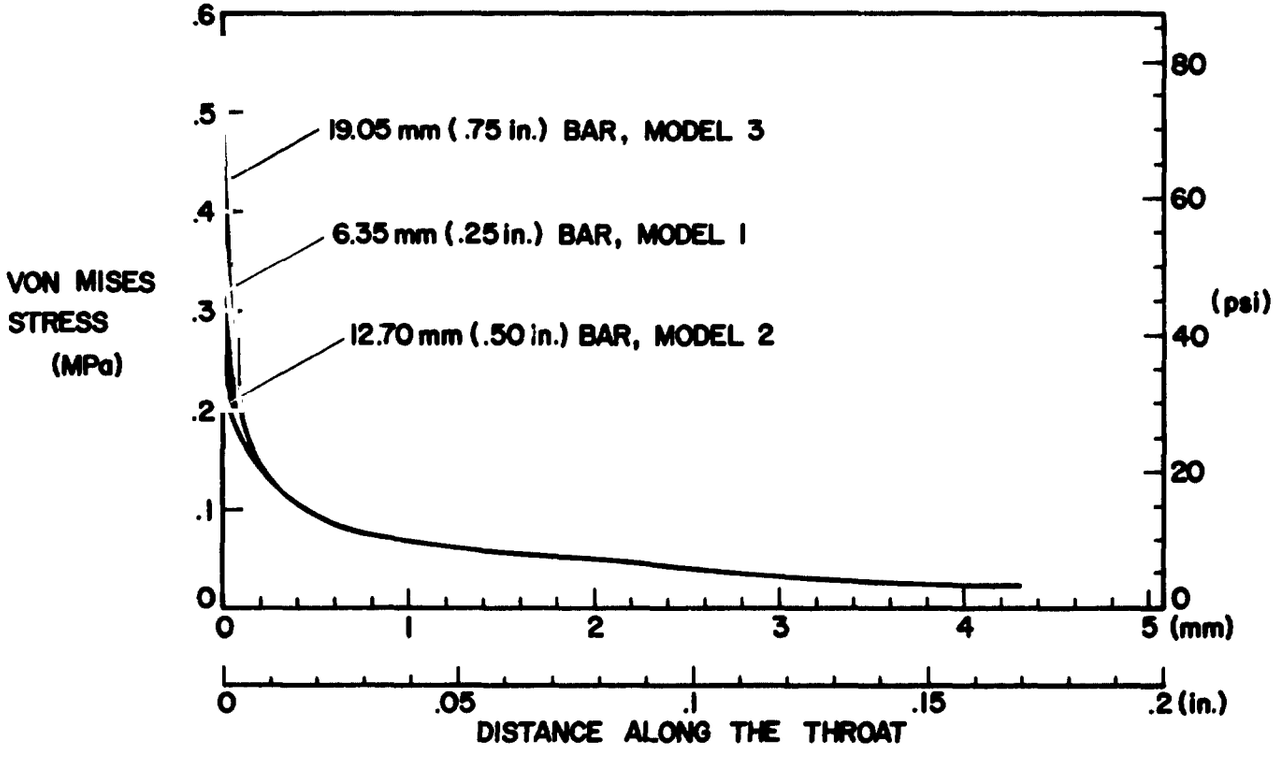

FIGURE 5 VON MISES STRESS ALONG THROAT, CASE I

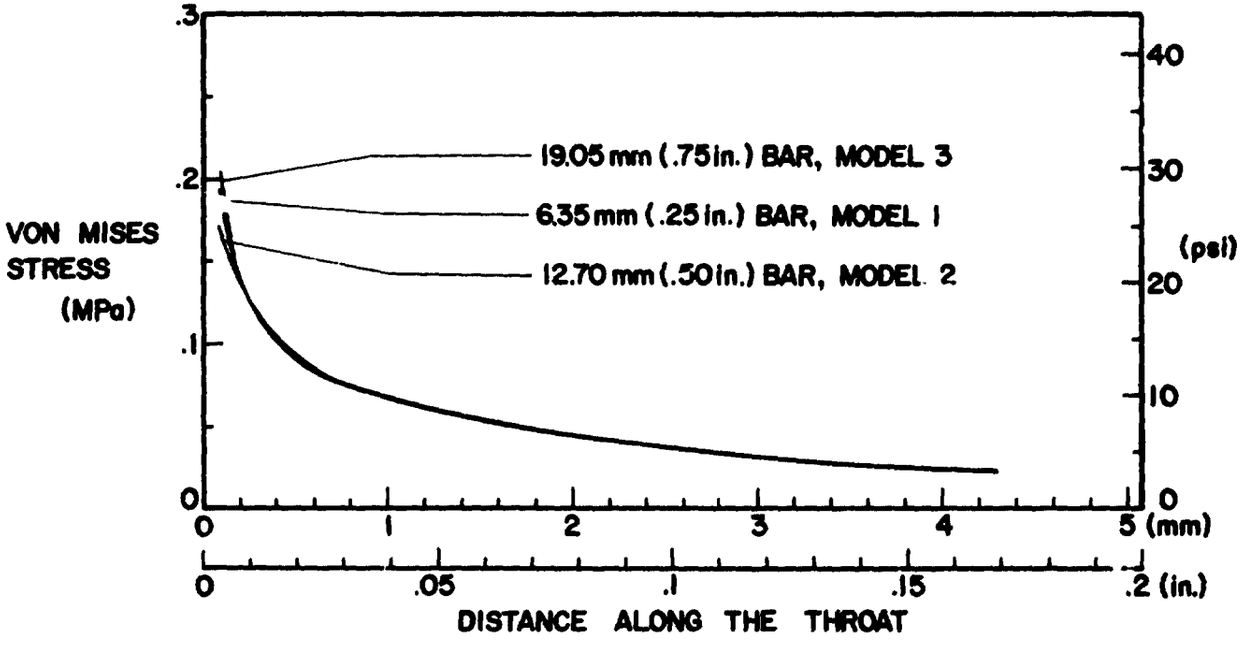

FIGURE 6 VON MISES STRESS ALONG THROAT, CASE 1 (EXPANDED SCALE)

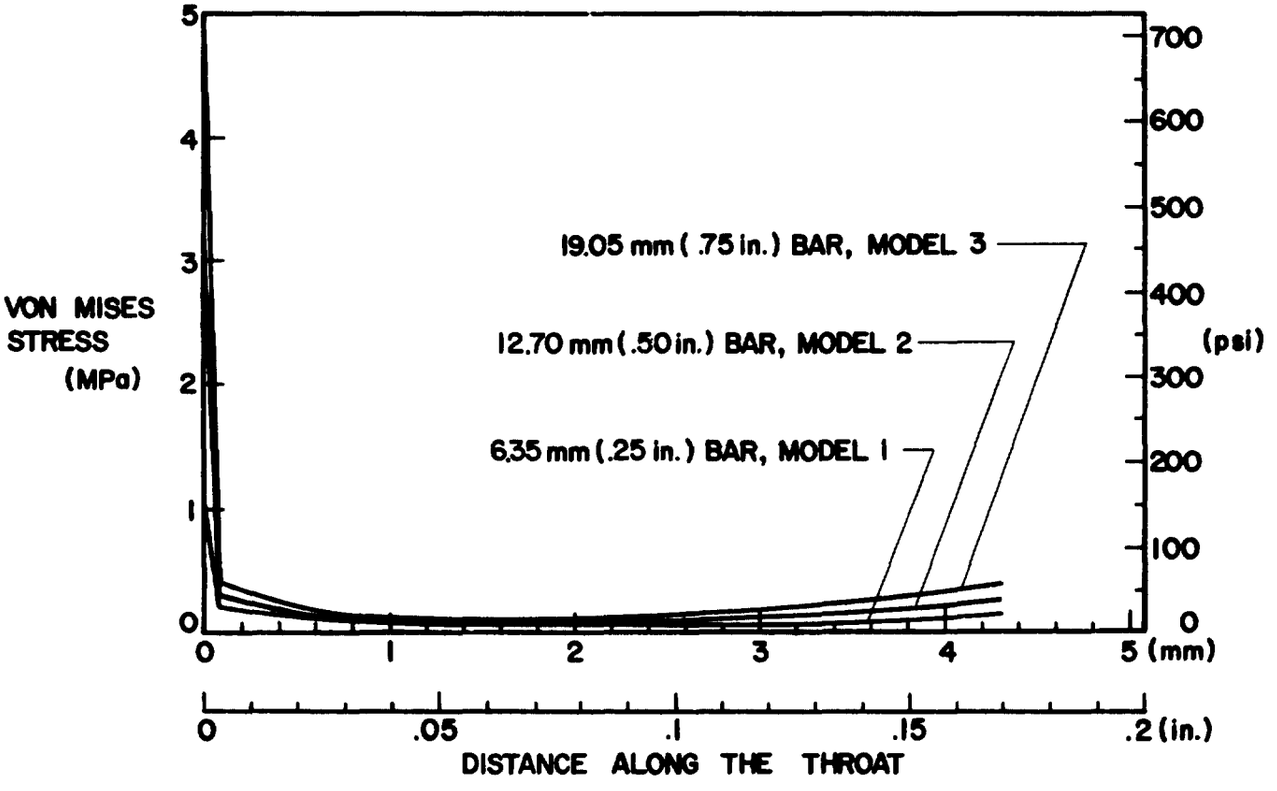

FIGURE 7 VON MISES STRESS ALONG THROAT, CASE 2

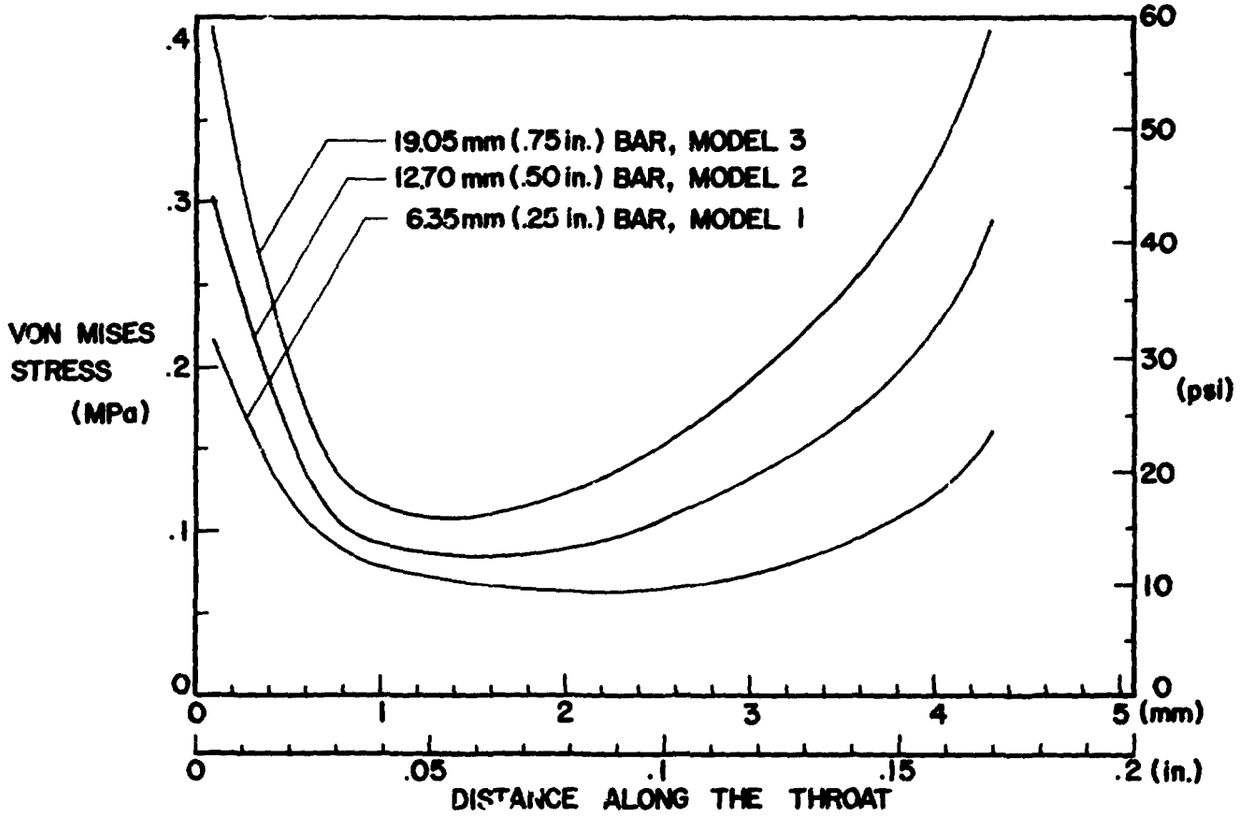

FIGURE 8 VON MISES STRESS ALONG THROAT, CASE 2 (EXPANDED SCALE)

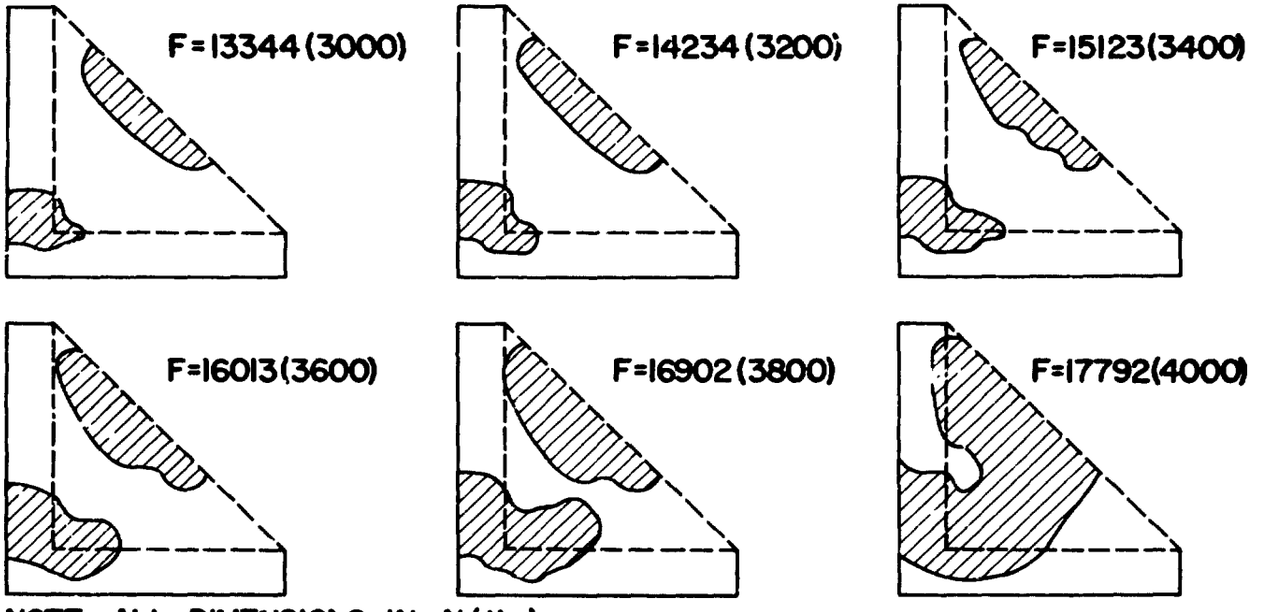

NOTE ALL DIMENSIONS IN N(lbs)

FIGURE 9 DEVELOPMENT OF PLASTIC INSTABILITY, MODEL 1, CASE 2

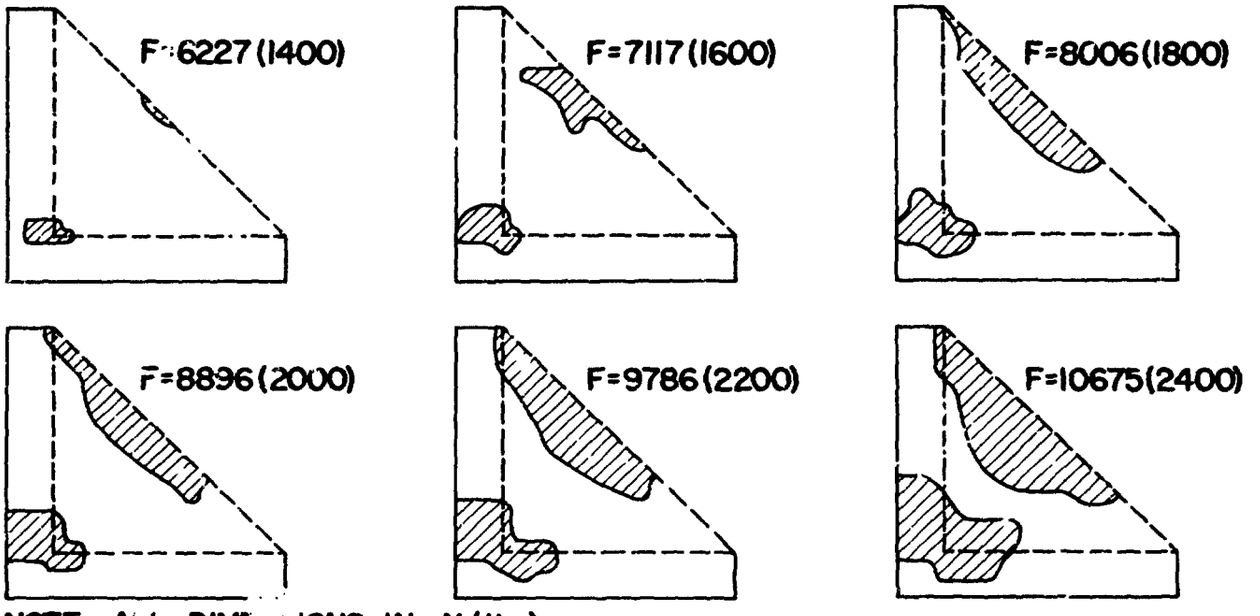

NOTE ALL DIMENSIONS IN N (lbs)

FIGURE 10 DEVELOPMENT OF PLASTIC INSTABILITY, MODEL 2, CASE 2

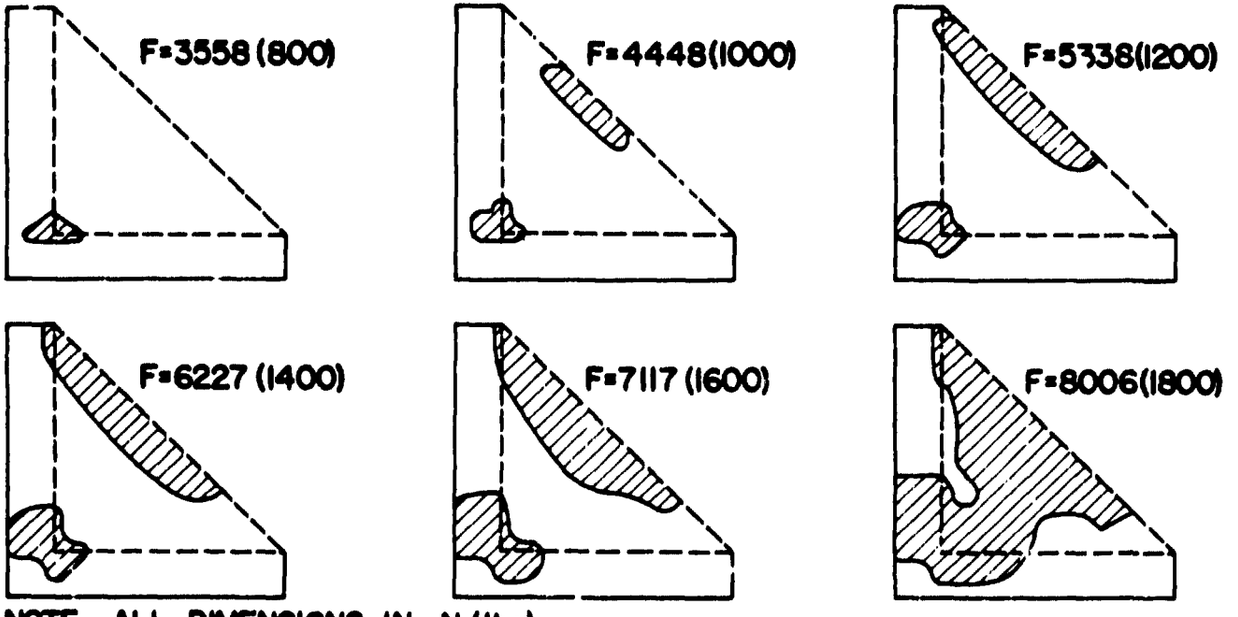

NOTE ALL DIMENSIONS IN N (lbs)

FIGURE 11 DEVELOPMENT OF PLASTIC INSTABILITY, MODEL 3, CASE 2

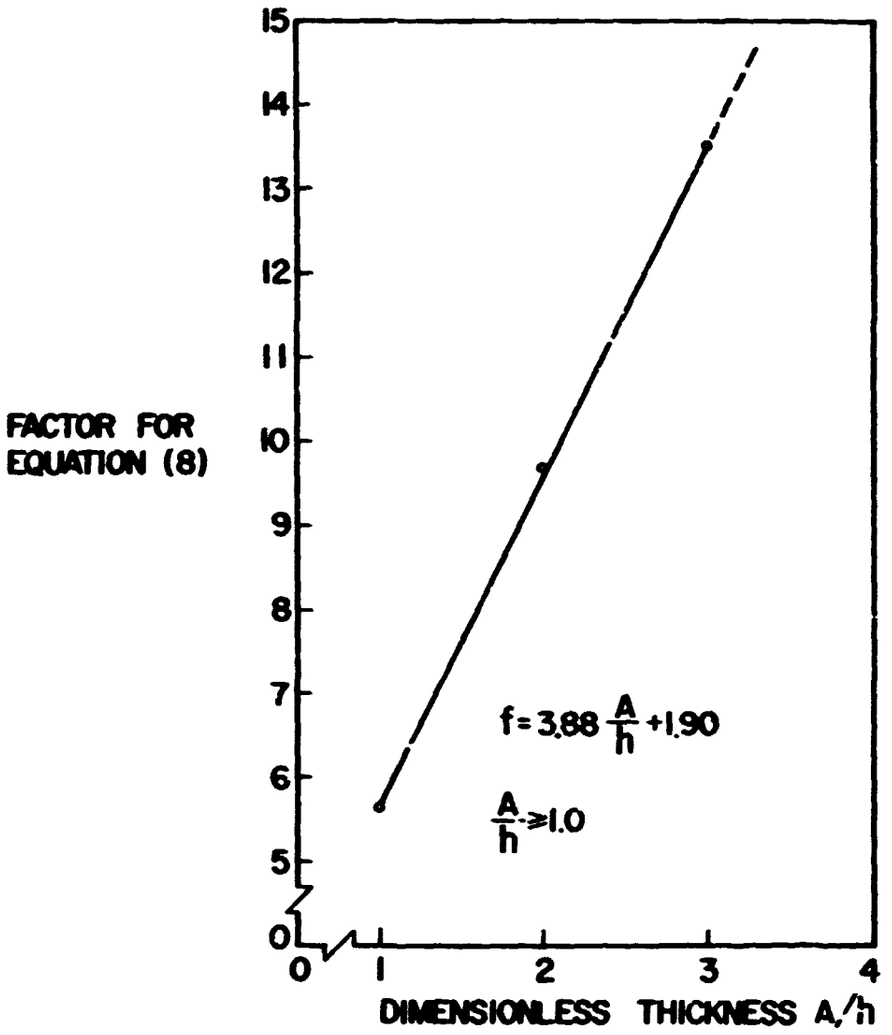

FIGURE 12 FACTOR FOR EQUATION 8